The University of Southern Mississippi
The Aquila Digital Community

Honors Theses | Honors College

5-2021

Effects of Static Mixer Geometry on Polyurethane Properties

Christian R. Dixon

Follow this and additional works at: https://aquila.usm.edu/honors_theses

 Part of the Polymer and Organic Materials Commons

Recommended Citation

Dixon, Christian R., "Effects of Static Mixer Geometry on Polyurethane Properties" (2021). *Honors Theses*. 796.
https://aquila.usm.edu/honors_theses/796

This Honors College Thesis is brought to you for free and open access by the Honors College at The Aquila Digital Community. It has been accepted for inclusion in Honors Theses by an authorized administrator of The Aquila Digital Community. For more information, please contact Joshua.Cromwell@usm.edu, Jennie.Vance@usm.edu.

Effects of Static Mixer Geometry on Polyurethane Properties

by

Christian Robert Dixon

A Thesis
Submitted to the Honors College of
The University of Southern Mississippi
in Partial Fulfillment
of Honors Requirements

May 2021

Approved by:

Jeffrey Wiggins, Ph.D., Thesis Advisor,
School of Polymer Science and Engineering

Derek Patton, Ph.D., Director,
School of Polymer Science and Engineering

Ellen Weinauer, Ph.D., Dean
Honors College

ABSTRACT

The field of additive manufacturing has gained significant academic interest in the past few decades with a recently developed type of three-dimensional (3D) printing. Reactive extrusion additive manufacturing combines precursor materials within a static mixer (SM) head, where polymerization begins before deposition. Variable static mixer geometries currently exist, but the relationship between mixer geometry and post-polymerization mechanical properties is undefined. To elucidate this relationship, a series of experiments with identical chemistry was performed using a high shear SM, a low shear SM, and a comparative batch reaction. While higher shear mixing trends with faster polymerization for step-growth polymerizations, consistent precursor chemistry is expected to yield identical polymer properties. Therefore, polyurethane conversion and viscosity-evolution were elucidated by performing Fourier transform infrared spectroscopy (FTIR) and rheology analyses. Post-polymerization thermomechanical properties were determined through dynamic mechanical analysis. Initially hypothesized that higher shear SM geometry would grant accelerated viscosity growth, the batch reaction achieved a storage-loss modulus crossover first, while the high shear rate optimixer (HSO) geometry had a faster crossover time than the low shear spiral (LSS). Post-polymerization properties remained fairly consistent, but some discrepancies arose, necessitating future studies to prove the root cause of the differences. The results in this research further additive manufacturing by systematically studying the influence of static mixer geometry on polyurethane properties.

Keywords: Thermoplastic Polyurethane, Ambient Reactive Extrusion, Shear

DEDICATION

I would like to give glory to God for giving us his only Son, and I dedicate my Honors Thesis to my father, who has gone before me.

ACKNOWLEDGMENTS

I sincerely thank my thesis advisor, Dr. Jeffrey Wiggins, for his involvement in my intellectual development, particularly the undergraduate research performed in his lab, and especially for the high academic standards he set for me. I additionally thank my graduate student, Aynslie Fritz, for her contributions and mentorship during this research.

I thank The University of Southern Mississippi for granting my admission to the top, and the Honors College for giving me this opportunity to soar. I thank Dr. Ellen Weinauer for expanding my academic possibilities, and Stacey Ready for organizing them. I thank the School of Polymer Science and Engineering for their instructions and support, as professors with deep care in student learning. I am grateful for sponsorship of my Engineering Capstone by the Director, Dr. Derek Patton. I additionally thank the undergraduate advisor, Dr. Heather Broadhead, for her contributions to my academic past and future. I would like to express gratitude for my benefactors, who have provided for me this wonderful opportunity.

Thank you, Mikhail, for motivating me as my big brother. Finally, thank you mom and dad, for raising me with love and to such high standards.

TABLE OF CONTENTS

LIST OF TABLES

LIST OF ILLUSTRATIONS

LIST OF ABBREVIATIONS

3D	Three-Dimensional
ARE	Ambient Reactive Extrusion
BAAM	Big Area Additive Manufacturing
CAD	Computer-Aided Design
CE	Chain Extender
DBTDL	Dibutyltin Dilaurate
DMA	Dynamic Mechanical Analysis
DoC	Degree of Conversion
FDM	Fused Deposition Modeling
FTIR	Fourier Transform Infrared Spectroscopy
HB	Hard Block
HSO	High Shear Optimixer
H_{12}MDI	4,4'-Methylenebis(Cyclohexyl Isocyanate)
IPDI	Isophorone Diisocyanate
LSS	Low Shear Spiral
1,4-BD	1,4-Butanediol
PTMEG	Polytetramethylene Ether Glycol
RT-FTIR	Real Time Fourier Transform Infrared Spectroscopy
SAOS	Small Amplitude Oscillatory Shear
SB	Soft Block
SLA	Stereolithography
SM	Static Mixer

TDI	Toluene Diisocyanate
Tg	Glass Transition Temperature
TPU	Thermoplastic Polyurethanes
UV	Ultraviolet

CHAPTER I: INTRODUCTION

Additive Manufacturing

Additive Manufacturing (AM), or 3D printing, differs from typical machining as products are fabricated layer by layer, rather than assembling pieces, or subtractive manufacturing where desired shapes are cut from blocks of material.[1] In AM, Computer-Aided Design (CAD) software that directs a printer on assembly instructions. Usage of CAD software gives AM two common characteristics, namely that models can be rapidly prototyped from an idea, and that CAD instructions can be easily shared or modified between computers. A sample CAD design of drum brakes can be seen in Figure 1.[2]

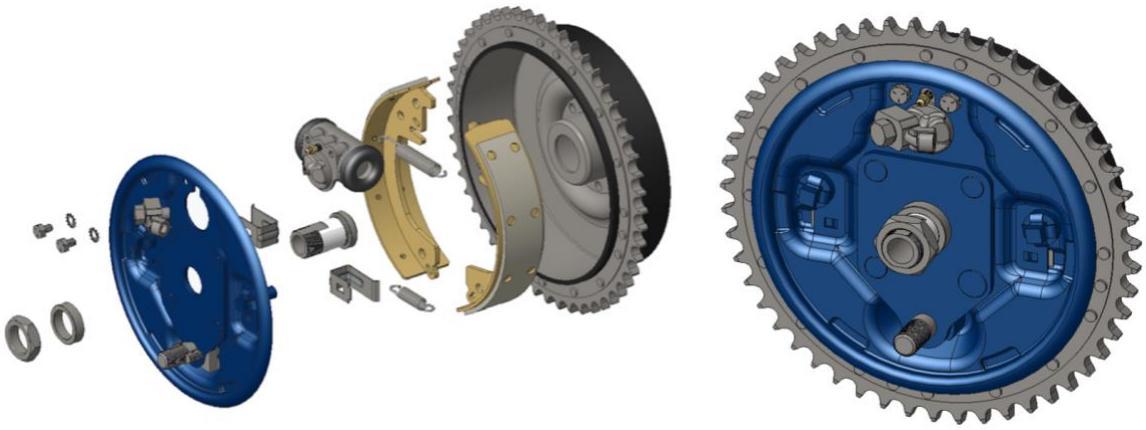

Figure 1. Modeling and Assembly of Car Brakes

To change the product shape, normal machining may require a specialized drill bit or a new mold, whereas AM can print a variety of complex shapes by changing the design instructions.[3] Demand for AM has increased in modern times, where computer networking has led to an era of product customization in response to increased customer review.[1] While many industries, such as automotive, have adopted AM for prototyping, AM still has setbacks that inhibit industrial scale production of products. Current

limitations include manufacturing speed, scalability, material selection, and part anisotropy.[3]

The earliest recorded 3D printing processes began in 1981 by Hideo Kodama.[4] Kodama's work was based on using ultra-violet (UV) lights to harden polymers through photo-initiation. This process was expanded by Charles Hull, inventor of what is now known as stereolithography (SLA).[5] A model SLA printer in which a focused UV laser initiates photoradicals in a resin tank, is displayed in Figure 2.[6] As AM expanded, there was a need to scale and modify objects as 3D models for SLA manufacturing, resulting in the development of CAD software. As the use of AM grew, the technique became popular for rapid prototyping as it did not require unique molds, tools, punches, or sanders. These requirements greatly reduced the cost of prototyping, as traditional prototyping requires a milling machine that can cost $500,000; conversely, a 3D printer could perform the same processes for $10,000.[7] A common problem restricting AM processes from being used outside of prototyping is manufacturing speed. Expanding a design to twice its original dimensions increases its volume by a factor of eight, proportionately affecting the build time. Limited by a single arm applying the entire layer, AM can be accelerated by increasing the distance between layers, or increasing the nozzle diameter, at a cost of reducing product resolution. A second limitation to AM is the scalability. A 3D printer can never print a product smaller than its base.[8] Printing large products therefore requires an expansive

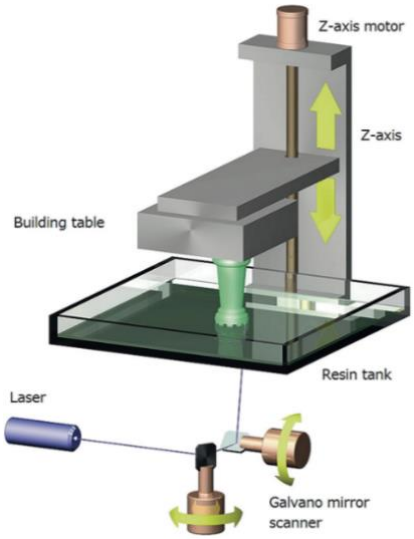

Figure 2. Three-Dimensional SLA Printer

floor space that limits production and increases costs. AM is also limited by material selection, determined by the processing technique. These material selections, such as SLA requiring photosensitive materials for polymerization and subsequent fabrication, will be discussed in more detail in their relevant sections.

Anisotropy represents the prime mechanical hindrance of AM that prevents it from utilization in mass production.[9] Anisotropic materials have non-homogeneous mechanical properties depending on the direction of an applied force. Composites are an example of anisotropic materials, as they retain tensile strength only when force is applied co-axially to the fiber. In AM, anisotropy is a flaw created by the fabrication process. For example, Big Area Additive Manufacturing (BAAM) relies upon heating polymerized pellets, which cool to solidify.[10] The interfaces between added layers have minimal chemical bonding without polymer chains stretching between them, separating easily in response to force. While a force that is co-planer with the layer is resisted, a tangential force rapidly divides layers.[9] Part anisotropy limits industrial applications of AM, as fabricated models cannot withstand pressure or bear loads. Anisotropy manifests distinctly in different AM processes; herein, anisotropy will be discussed across different AM methods.

Fused Deposition Modeling

Possibly the most common type of AM and most universally recognized is Fused Deposition Modeling (FDM), which operates by heating and applying a filament of polymerized material, allowing it to cool and solidify (Figure 3).[11] While FDM excels in manufacturing at a low cost, its disadvantages are tied to its manufacturing process.

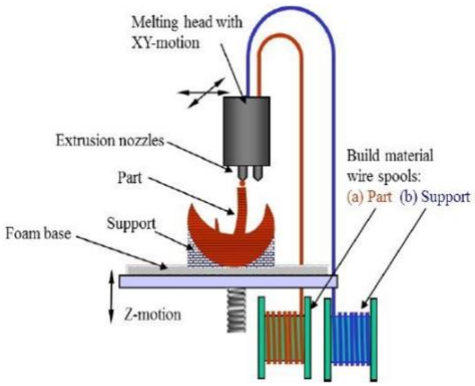

Printer Diagram

First, it is significantly limited in material selection. As the filament must be heated past its melting point, FDM material selection is limited to thermoplastics. Additionally, the melted polymer must have a viscosity suitable for the width of the nozzle head. A nuisance of FDM is that complex parts with overhanging sections often require temporary scaffolding to be printed to support the part.[12] These scaffolds waste material and require time for removal in post processing, which is still typically done by hand. However, waste is still 40% smaller when compared to subtractive machining technologies.[7] Additionally, resolution is limited to nozzle diameter, and the smaller the diameter the finer the detail, but the longer the print time. A final limitation of FDM lies within the fabrication of materials with poor mechanical properties.[13] Filaments are pre-polymerized, and layers of materials are only held by few bonds without any polymer chains stretching between them, as the filaments are merely fused together. Therefore, forces applied perpendicular to the plane of print build easily shear the printed layers apart, while parallel forces are far more resisted. While the concern of anisotropy can be relaxed by proper build orientation, the final product will still have a plane on which it is weak to applied force.[9] This means FDM is limited to prototyping and has no current application in high performance materials. Alternative AM methods attempt to address these concerns.

Stereolithography

An additional AM method is stereolithography (SLA), where a model is fabricated by curing a resin in layers using an ultraviolet (UV) laser beam.[5] The polymer resins are stored as low viscosity materials; use of a photocatalyst yields crosslinking and formation of thermoset polymers upon exposure to UV. The UV laser targets the mold as directed by the CAD software, and upon a layer being completed, the part is raised off the bed of resin to add successive layers. Each layer is typically 0.05 mm to 0.15 mm thick, with smaller distances increasing resolution and build time.[14] SLA has several advantages, such as its printing speed. Depending upon print size, layer thickness, and part complexity, fabrication can last as little as a few hours, or up to one day.[4] The material cost associated with SLA is low as very cheap photopolymer resins are used. Scaling is also simple, as CAD designs can be easily manipulated to increase dimensions while maintaining the original proportions. Using photosensitive resin limits SLA fabrication.[5] The resin must be secluded from ambient UV radiation provided by sunlight or incandescent bulbs within the working environment. Exposure to UV radiation will prematurely initiate radical polymerization, spoiling the stock before use. Stereolithography additionally has a limited selection of materials, only using polymers which can be photopolymerized and excluding thermoplastic materials. Despite these limitations, SLA imparts minimal anisotropy, as the reactive nature permits successive layers to terminate in semi-polymerized chain

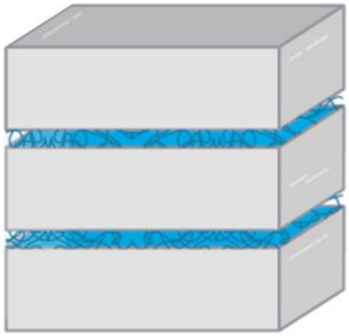

Figure 4. Stereolithography

Chemical Potential

ends, allowing chemical bonds to form that connect polymer chains between layers (Figure 4).[6]

Ambient Reactive Extrusion

Building upon the advantages found with FDM and the reactive nature of SLA to yield isotropic parts, a new AM method from Oak Ridge National Laboratory was recently introduced: Ambient Reactive Extrusion (ARE).[15] To manufacture polymerized parts, ARE requires specific chemorheological properties from the starting materials. In ARE, layers are added by mixing low viscosity precursor materials prior to deposition. Reactive materials are drawn from separate containers and mixed in a static mixer (SM), polymerizing upon deposition. Precursor materials flowing through the mixhead must have a low viscosity to function as processible liquids, relying upon rapid kinetics to build dimensional stability when deposited. Previous layers must achieve dimensional stability at low conversion rates, allowing them to act as a foundation for succeeding layers while retaining the chemical potential to bond with them. Anisotropy can be reduced as layers are bound by sharing chemical bonds and polymer chains, as opposed to comparative AM processes where intermolecular forces bind layers.[9]

This research focused on Ambient Reactive Extrusion and elucidated the effects of static mixer design on the chemorheological and thermomechanical properties of polymers to expand the material selection of AM to new polymers. To characterize the effect of mixing on curative properties, a series of experiments were performed using a high shear SM and a low shear SM, compared to a baseline batch reaction. Each synthesis was conducted using identical chemistry, with only mixing shear varied across samples. A helical low shear spiral (LSS), and a non-helical high shear optimixer (HSO)

were employed, as detailed in the Materials section. It was predicted that static mixer geometry for use in Ambient Reactive Extrusion (ARE) could be modified by adjusting shear rate to increase viscosity growth during polymerization and to expand the applications of Additive Manufacturing.[16]

Ambient Reactive Extrusion of Thermoplastic Polyurethanes (TPUs)

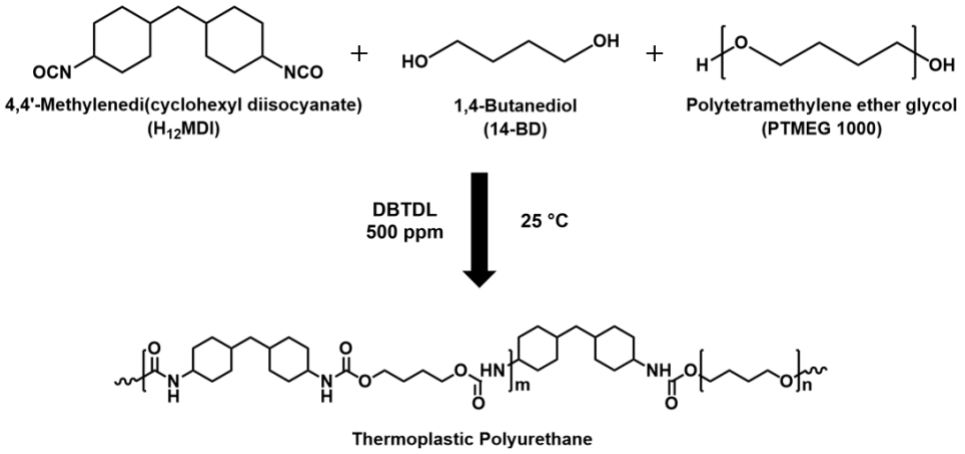

Figure 5. Model TPU Polymerized from H_{12}MDI, 1,4-butanediol, and PTMEG 1000

Urethane linkages are formed when an isocyanate reacts with a hydroxyl group, as shown in Figure 5.[17] Typically, polyurethanes are synthesized via step growth polymerization of a diisocyanate monomer with a high molecular weight polyol and a shorter diol. Urethane bonds along the backbone of polyurethanes result in strong intermolecular hydrogen bonding.[18] Diisocyanate reactions with long polyols result in Soft Block (SB) regions with increased distance between the urethane linkages. The shorter diols lead to sections of high urethane bond density, which assemble into Hard Block (HB) domains. The short diol is also known as a Chain Extender (CE), as it increases the block length of the HB region. Polyurethanes are therefore highly customizable materials, as the elastomeric behavior resulting from the crystalline and

amorphous regions is tunable via HB to SB ratio. Additionally, the hydrogen bonding between urethane groups can be heated to disassociate, unlike covalently bonded crosslinking.[17] Heating these bonds allows chains to flow and be molded to any shape, demonstrating elastomeric behavior again once cooled. The hydrogen bonds result in polyurethanes quickly building mechanical strength and viscosity upon polymerizing, which is relevant to the chemorheological requirements of ARE.

CHAPTER II: EXPERIMENTAL

Materials

The diisocyanate employed for the TPU was 4,4'-methylenebis(cyclohexyl isocyanate) (H_{12}MDI) (TCI Chemicals, Mn = 262.35 g/mol). The hydroxyl terminated materials of 1,4-butanediol (1,4-BD) (Sigma Aldrich, Mn = 90.12 g/mol) and polytetramethylene ether glycol (PTMEG) (Aldrich, Mn = 1000 g/mol) were combined with the catalyst, dibutyltin dilaurate (DBTDL) (TCI Chemicals), to be dried under vacuum at 70 °C for at least 3 hours prior to use.

Polyurethane Synthesis

All batch and ARE polyurethanes were formulated using an unmodified blend, with a 50:50 wt% HB:SB ratio, with 500 ppm catalyst. Each TPU additionally had an isocyanate index of [NCO]/[OH] = 1.03. The diisocyanate was added in slight excess, as its high reactivity would lead to monomer loss from side reactions. By preparing an excess of diisocyanate, the reaction mixture would lose monomer concentration and fall to the intended stoichiometry. Batch samples were prepared by placing the appropriate amount of diisocyanate within a flame-dried scintillation vial at room temperature. A separate flame-dried vial was then filled with the proportionate catalyst, polyol, and diol in that order. Vials were flame dried to purge water vapor from the container, which would promote side reactions with the diisocyanate. The diisocyanate was then added to the vial containing hydroxyl group compounds and stirred with a glass stir rod for 15 seconds, until being placed on its relevant characterization instrument.

ARE Platform and Static Mixer Geometry

For ARE, a lab-scale continuous static mixer reactor was devised. Synthesis was prepared by depositing the relevant amount of diisocyanate within a flame-dried round bottom flask, with a second dried round bottom flask containing the equivalent amounts of catalyst, polyol, and diol. The ARE platform was therefore a two-component setup, with flask 1 on the left containing the compounds with hydroxyl functionalities and the catalyst, and flask 2 on the right containing the diisocyanate monomer, as shown in Figure 6.

Figure 6. Ambient Reactive Extrusion Platform Setup

The materials in the flasks were fed through separate pumps into the static mixer, where polymerization began. Both flasks were continuously stirred at 30 °C. Samples were received directly from static mixer output, with a consistent 15 second delay between reception and characterization. Prior to each synthesis, the pumps were individually calibrated to feed rates that reproduced the desired stoichiometry for each sample. Feed rates in grams per minute were approximated by measuring the output of each trial for 15 seconds and multiplying by four. The manifold connected to the SM had an additive output, meaning it would combine the feed rates of both inputs. Feed rates were then plotted in a calibration curve (Figure 7) to discern a pair of settings that would most closely meet the desired stoichiometry.

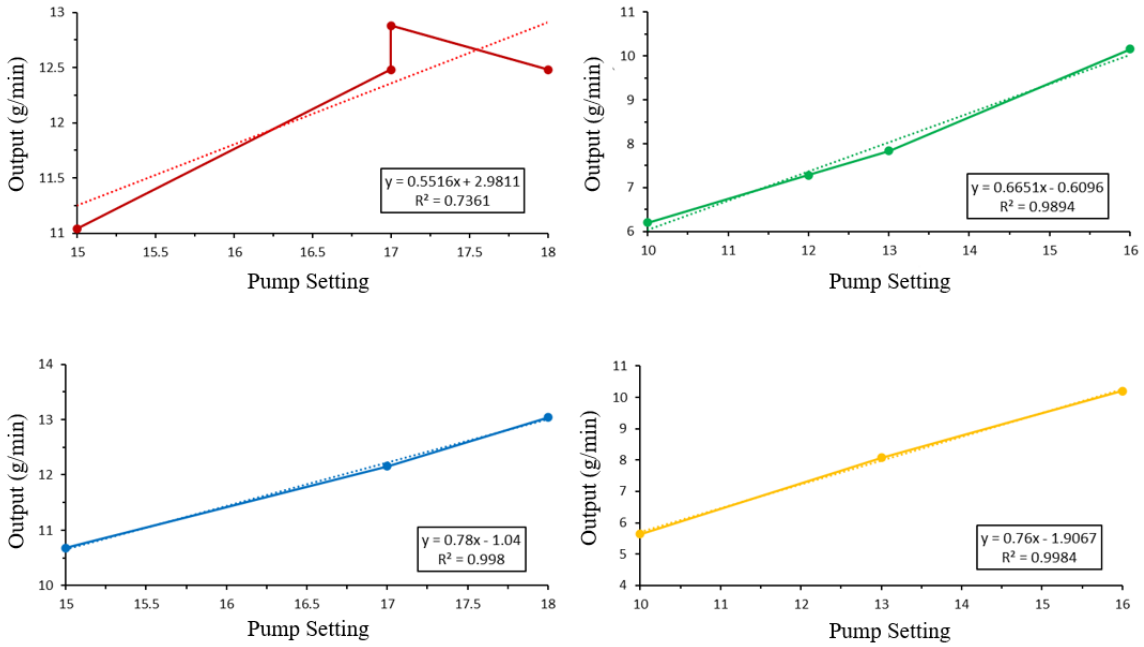

Figure 7. Top Left: Spiral Pump 1 Curve. Top Right: Spiral Pump 2 Curve. Bottom Left: Optimixer Pump 1 Curve. Bottom Right: Optimixer Pump 2 Curve.

Pump 1 fed its respective flask with compounds that contain hydroxyl functionalities for the LSS and HSO at 11.04 g/min and 12.16 g/min, respectively, at respective settings 15 and 17. Pump 2 fed the diisocyanate monomer for the LSS and HSO at 7.28 g/min and 8.08 g/min, respectively, at respective settings 12 and 13. All data fitted to calibration curves were recorded in Table 1. The intended mass ratio was 1:1.56 diisocyanate to hydroxyl, with the LSS having a recorded ratio of 1:1.52 and the HSO being recorded as 1:1.50. While the experimental values deviated slightly from intended stoichiometry, the diisocyanate excess was preserved.

Table 1. Pump Calibration Mass Output vs. Time

Platform	Combined Settings	Expected Output (g/min)	Recorded Output (g/min)
Spiral	15 & 12	18.32	16.78
Optimixer	17 & 13	20.24	21.04
Spiral Pump 1		**Spiral Pump 2**	
Setting	Output (g/min)	Setting	Output (g/min)
15	11.04	10	6.20
17	12.48	12	7.28
17	12.88	13	7.84
18	12.48	16	10.16
Optimixer Pump 1		**Optimixer Pump 2**	
Setting	Output (g/min)	Setting	Output (g/min)
15	10.68	10	5.64
17	12.16	13	8.08
18	13.04	16	10.20

The LSS mixers (Nordson EFD part number 7700837) were provided by Brandywine Materials; specifications: length of 22.45 cm, element diameter of 2.54 mm, an outlet tip orifice of 2.29 mm, containing 24 spiral elements. The HSO mixers (Nordson EFD part number 7361695) were likewise provided by Brandywine Materials; specifications: with 25 mixing elements, but with a length of 13.00 cm, an element diameter of 8.7 mm, and an outlet tip orifice of 1.78 mm.

Real-Time Fourier Transform Infrared Spectroscopy (RT-FTIR)

A Perkin Elmer Frontier IR in transmission mode performed in-situ tracking of the polyurethane reaction progress within the spectral range of 600 to 4000 cm^{-1} using a 10° Pike Technologies transmission accessory with NaCl plates, under ambient conditions. IR spectra were collected continuously throughout the reaction for 6 hours at an average of ~11 s per scan, co-averaged over 10 scans at 2 cm^{-1} resolution. Peaks

indicative of polyurethane polymerization were normalized to the aliphatic peak at 780 cm^{-1}: 3500 cm^{-1} (primary hydroxyl), 3300 cm^{-1} (secondary amine), and 2260 cm^{-1} (isocyanate). Polymerization degree of conversion was calculated using Equation 1.

$$DoC = \frac{(\frac{A_{2260}}{A_{780}})_0 - (\frac{A_{2260}}{A_{780}})_t}{(\frac{A_{2260}}{A_{780}})_0} * 100\% \quad \text{Equation 1}$$

Rheology

Rheological characterization was performed using a TA Instruments ARES G2 Rheometer equipped with a forced convection oven on 25 mm aluminum parallel plates. Small amplitude oscillatory shear (SAOS) experiments were performed on each sample employing an angular frequency of 10 rad/s and 0.5% strain at 25 °C.

Dynamic Mechanical Analysis

Dynamic mechanical analysis (DMA) was utilized to observe the storage modulus, loss modulus, and glass transition temperature (Tg) of the polyurethanes on a TA Instruments Q800 DMA in tensile mode. Samples were equilibrated at -120 °C, then ramped 3 °C/min to 125 °C. A peak in Tan Delta is observed as a Tg.

CHAPTER III: RESULTS

Alternative TPU Synthesis

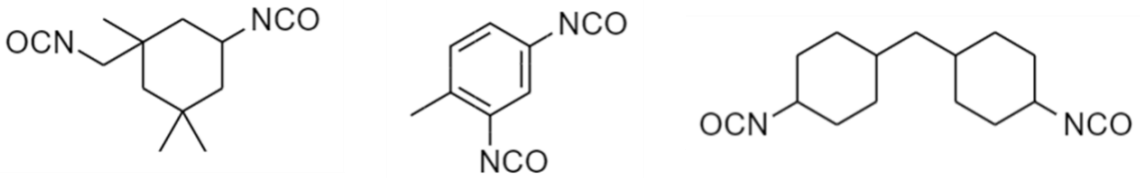

Figure 8. Middle: Toluene *Diisocyanate*

Left: Isophorone Diisocyanate. Right: 4,4'-Methylenebis(Cyclohexyl Isocyanate).

Several syntheses of polyurethanes were performed until one suitable for ARE was fashioned (Figure 8). For the diisocyanate monomer, isophorone diisocyanate (IPDI) was first investigated, as it is liquid at room temperature, which eased processing. It was found to have too slow of a cure rate, taking six hours to achieve a crossover. Being an aliphatic monomer, it lacked the ability to delocalize a negative charge around the aromatic ring, making the isocyanate more nucleophilic towards the hydrogen in the alcohol.[19] Additionally, IPDI is asymmetric, with the dibutyltin dilaurate catalyst disfavoring the primary isocyanate, further inhibiting the reaction rate.[20] As a symmetric and aromatic diisocyanate, toluene diisocyanate (TDI) synthesis was then attempted. During sample preparation TDI built viscosity so quickly that it entrapped air. Additionally, samples were crystalline and brittle, prone to fracture while being prepared. Excessive crystallinity was caused by the presence of aromatic rings along the backbone, where pi bonds would allow chains to order and densely pack.[19] Finally, as a symmetric and aliphatic diisocyanate, H_{12}MDI was chosen, which had a sufficient reaction rate higher than IPDI, and displayed properties that did not impede sample preparation like TDI did. Additionally, H_{12}MDI is liquid at room temperature, which eased processing.

Reaction Progression of Polyurethane Samples

The degree of conversion (DoC) throughout the polymerization will play an important role for ARE printing, as it will control the degree of interlayer polymerization, and thus, anisotropy, of printed specimens. For this reason, real-time Fourier transform infrared spectroscopy (RT-FTIR) was utilized to track the reaction progress. Resulting RT-FTIR spectra revealed that, while the low-shear spiral static mixer (LSS) and high-shear optimixer static mixer (HSO) polyurethane spectra were similar, the polyurethane prepared through batch mixing had an increase in hydroxyl functionality as the reaction progressed, as shown in Figure 9. It is well established that diisocyanate reacts with

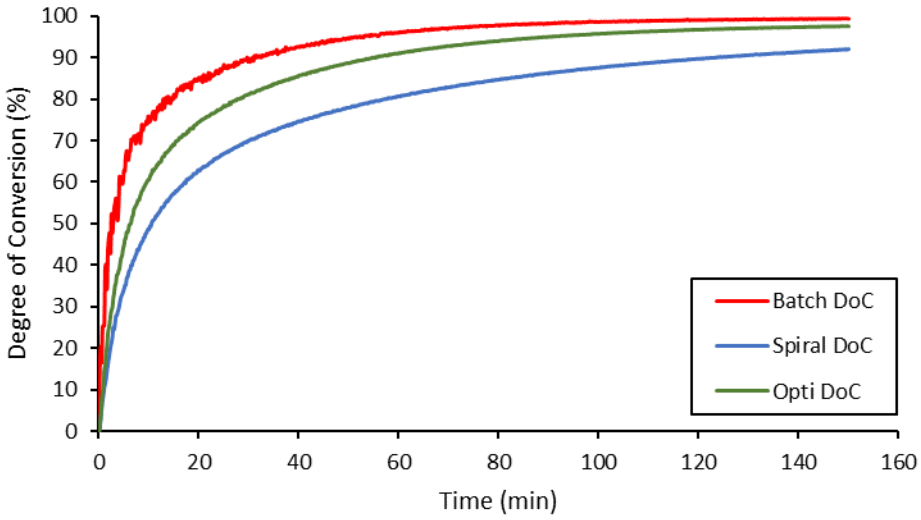

Figure 9. Comparative Degree of Conversion over 2.5 Hours

alcohol functionalities, resulting in decreasing peaks of both, which indicates consumption. However, the batch sample uniquely showed an increased hydroxyl presence as the reaction progressed, potentially indicating that side reactions resulted in consumption of diisocyanate monomer without full consumption of the polyol and CE.

This conclusion was further supported by a waxy residue that remained on polyurethane samples prepared through batch mixing.

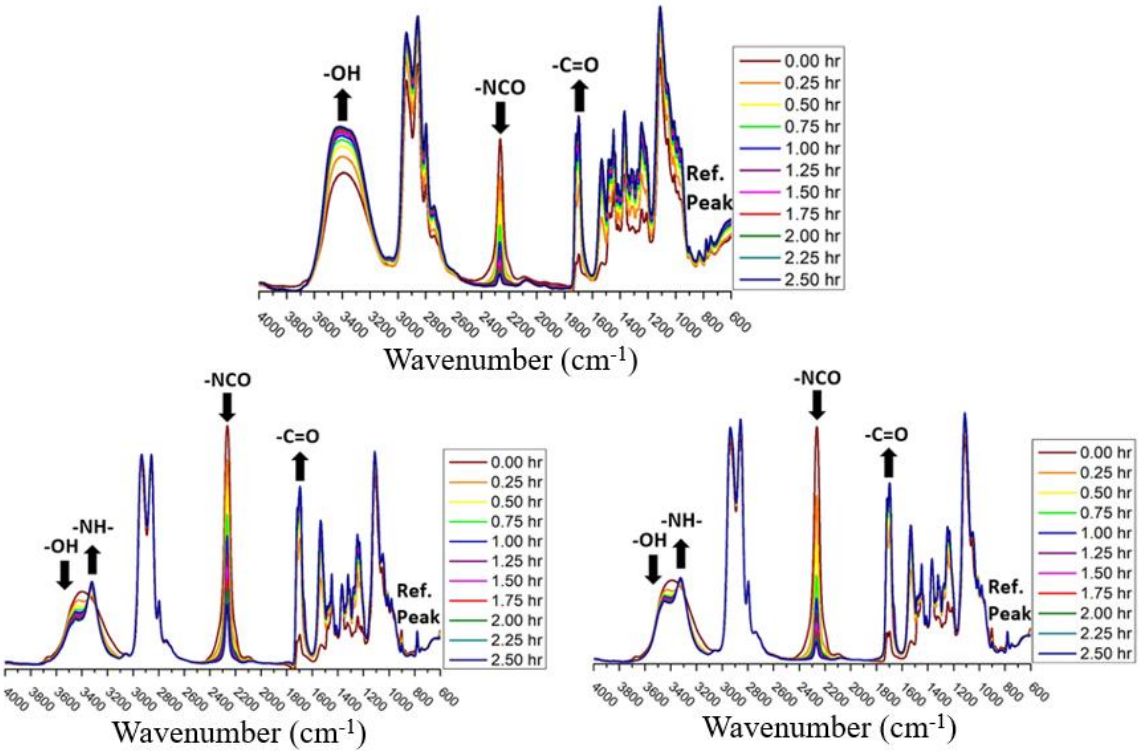

Figure 10. Top: Batch Mixing FTIR Spectra.

Bottom Left: Spiral SM FTIR Spectra. Bottom Right: Optimixer SM FTIR Spectra.

When examining all three spectra, a decrease in isocyanate functionality as the reaction progressed is observed. Additionally, all spectra demonstrated the increase in carbonyl presence, which implies the creation of urethane bonds where they are present (Figure 10). Additionally, all samples showed an increase in N-H bonds, which would be formed within urethane linkages. While LSS and HSO showed distinct N-H peaks, the batch sample revealed only a shoulder on the hydroxyl hump, potentially indicating less urethane formation and side reactions, as evidenced by near total consumption of isocyanate. Through tracking of the isocyanate peak and utilizing Equation 1, the degree

of conversion can be calculated. The batch polyurethane presented the highest degree of conversion, achieving 99.3% at 150 minutes. The HSO achieved the second highest DoC of 9.4% at 150 minutes, with LSS only reaching 92.0% at 150 minutes. It was initially hypothesized that higher shear would lead to higher DoC, however, the batch mixing was dynamic mixing compared to the passive mixing found within the LSS and HSO, potentially driving the higher consumption of isocyanate. It is also possible that the dynamic mixing of the batch reaction resulted in air, which contains water, being whipped into the sample. This, in turn, could result in side reactions that may explain the unexpected results.

Chemorheological Properties

The trend observed in the degree of conversion, with batch mixing providing the highest DoC, followed by HSO, then LSS, was established again in the chemorheological properties. Figure 11 provides the storage and loss moduli versus time of the batch mix (top), LSS (middle), and HSO (bottom). The batch

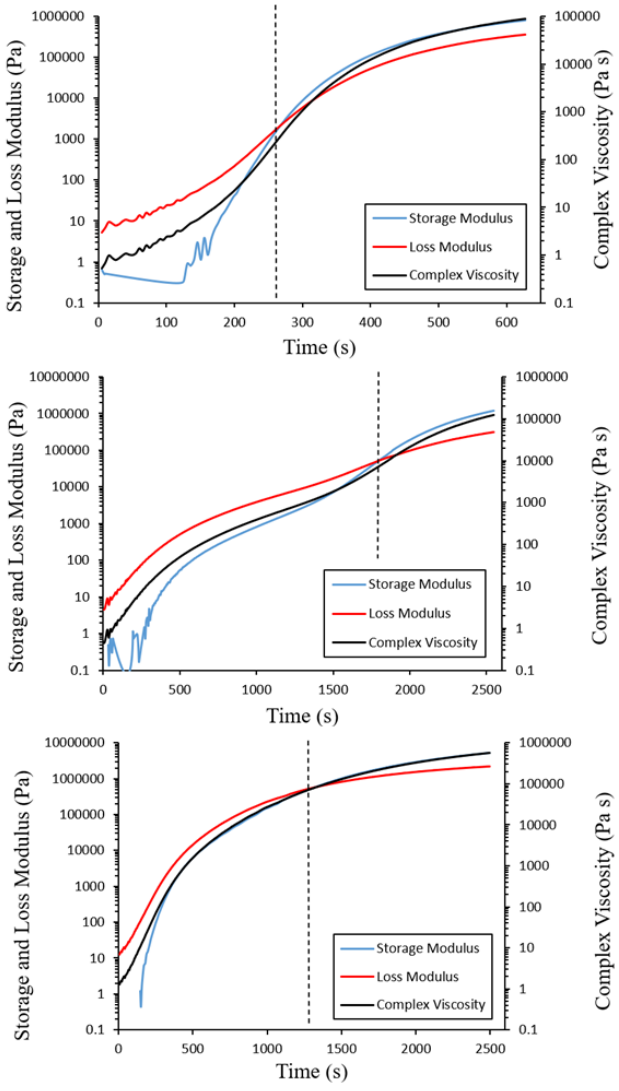

Figure 11. Top: Batch Rheological Data. Middle: Spiral Rheological Data. Bottom: Optimixer Rheological Data.

mixing polyurethane built storage modulus the fastest, achieving a crossover earlier than the other samples. It was followed by the HSO sample, with the LSS sample having the slowest crossover. The batch reaction achieved a crossover at 4.5 minutes, with HSO achieving a crossover at 21.1 minutes, and LSS achieving a crossover at 29.9 minutes. The initial hypothesis was that higher shear would result in better mixing, and thus, a faster reaction rate. However, the initial hypothesis did not account for the difference between dynamic and passive mixing, with the dynamic mixing providing faster reaction rates than SM. Directly comparing the rate of storage modulus growth across samples shows the same order of progression, as shown in Figure 12.

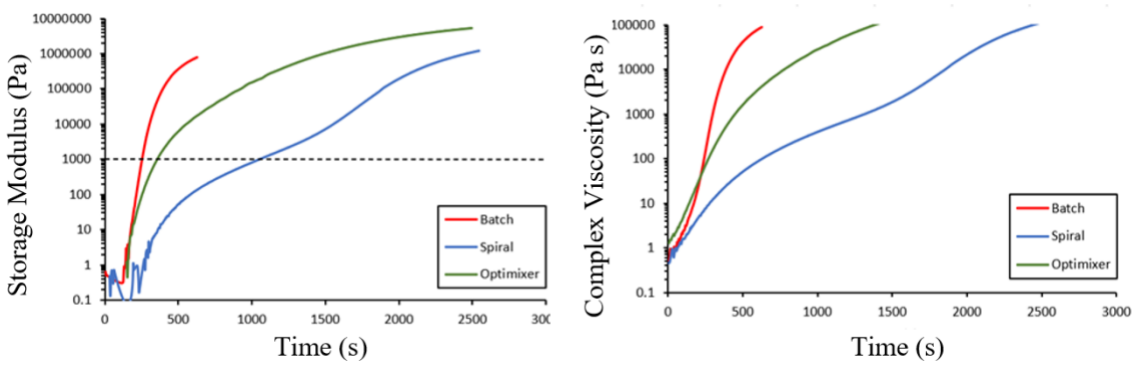

Figure 12. Left: Comparative Storage Modulus. Right: Comparative Complex Viscosity

The batch sample achieved dimensional stability fastest by reaching the critical storage modulus of 1000 Pa at 4.2 minutes, followed by the HSO sample (5.9 minutes); the LSS sample, again, was slowest at 17.6 minutes. Juxtaposition of Complex Viscosity as shown in Figure 12 likewise repeats the trend that the batch sample increased in viscosity the fastest, followed by the HSO, with the LSS being the slowest. When examining the differences in crossover time and reaching critical storage modulus, keeping ARE printing in mind, it is especially interesting that the HSO and LSS provide

approximately a 10-minute difference. For the design of an ARE process, this trend demonstrates that static mixer geometry, namely the difference in shear level, can influence the chemorheological properties of the sample. It is also possible that the batch mixing promoted side reactions which play a role in the significantly faster crossover time. Additional, future experiments would need to address potential side reactions in the batch reaction.

Thermomechanical Characterization

Storage modulus and glass transition temperature (Tg) were characterized by dynamic mechanical analysis (DMA). Juxtapositions of Tg peaks across various shears were conducted to elucidate the relationship between shear and thermomechanical curative properties. Glass transition temperatures were observed as peaks in Tan Delta, as displayed in Figure 13.

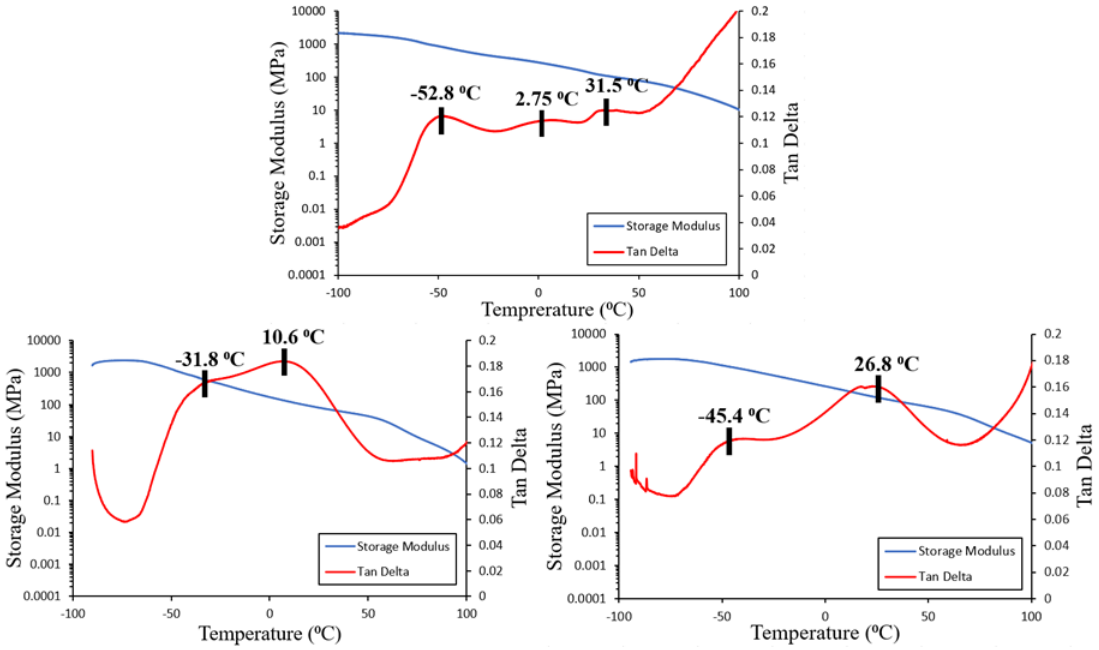

Figure 13. Dynamic Mechanical Analysis Results.

Top: Batch mixing. Bottom Left: Spiral SM. Bottom Right: Optimixer SM

The first Tg, ranging from -52.8 °C to -31.8 °C, indicates a soft block region of nearly unreacted polyol, as the Tg of pure PTMEG 1000 is 83 °C.[21] The next Tg demonstrated by all samples ranged from 10.6 °C to 31.5 °C. This higher glass transition temperature is indicative of the hard block Tg. Following Tg peaks, the last trend shared across samples was the large uptick in Tan Delta around 60 °C, albeit with LSS having a delayed onset. A large increase Tan Delta is a result of the sample yielding at this temperature, reflecting increased PU chain mobility as hydrogen bonds dissociated.[18] Finally, the batch trial demonstrated an additional Tg unrecorded in other samples, with a slight peak at 2.75 °C. This peak, distinctly above the polyol Tg while occurring beneath the hard block Tg, indicates a more heterogeneous microphase separation, with scattered HB elements entrapped within the SB.[22] Poor microphase separation was additionally demonstrated by broad Tg peaks in all samples, exhibited most prominently by the LSS spiral sample, where the -31.8 °C Tg_{SB} was displayed as a shoulder of the broad 10.6 °C Tg_{HB}.

Collectively, the DMA data suggests that no samples had explicit HB or SB regions, but rather heterogeneous domains where SB segments were entrapped within a majority HB, and vice versa. Inhomogeneous microphase separation occurs typically with TPUs, while processing methods, monomer selection, and fluorination can optimize domain clarity.[23] The method of polymerization employed for this research promoted poor microphase separation. In the one-shot method, all reacting material is mixed simultaneously, creating polymer chains with randomized structures. Conversely, a two-shot method consists of forming a prepolymer of the soft segment by end-capping it with excess diisocyanate monomers. After the prepolymer is formed, the short chain diol is

added, creating polyurethane chains that more closely follow a repeated pattern. The preparation method employed in this research more closely follows the one-shot method, resulting in the heterogeneous HB and SB domains.

CHAPTER IV: CONCLUSION

The initial hypothesis for this research was that higher shear static mixer would result in accelerated reaction rates and viscosity growth. While the results show that the high shear static mixer (HSO) did demonstrate accelerated viscosity growth and a faster reaction rate than the low shear static mixer (LSS), the batch reaction reached a higher degree of conversion after 2.5 hours and a storage-loss modulus crossover faster than either SM. Additionally, post-polymerization properties such as viscosity remained consistent across samples, with deviation occurring in RT-FTIR spectra. This project is therefore open to future studies to distinguish between the active shear of the batch preparation and the possible intrusion of side reactions.

CHAPTER V: FUTURE WORK

Future experiments could be designed to distinguish and identify different sources of error experienced in this research. While the HSO provided higher reaction rates than the LSS, the batch reaction demonstrated the fastest rate, likely due to side reactions with water because of the mixing method. To isolate the notions that active shear promotes reaction faster than passive shear, and that the active shear introduced side reactions, the synthesis portion could be repeated with different methodology. In addition to juxtaposing batch, LSS, and HSO samples, tests could be conducted where materials extruded from the static mixers would be stirred with a glass stir rod for 15 seconds. If the samples combining both shear methods demonstrated similar results as the batch reaction, then the increase in conversion and reaction rates promoted by the batch reaction are due to the active mixing method. If the hybrid samples followed the trends presented in this work, then the active mixing of the batch methodology promotes reaction faster than passive mixing. While care was taken to prevent the reaction of diisocyanate with moisture, such as vacuum sealing and flame drying, spectroscopic data suggests the presence of side reactions. To further limit the presence of moisture, DMA samples could be prepared in a glove box and compared to the samples fabricated in the fume hood. As the side reaction of diisocyanate with water yields a urea bond, results of future experiments could then be characterized with C-NMR, as urethane linkages contain a C-O bond that is not present in urea. Controlling for active shear and the presence of water vapor would allow for characterization of the results of this research, establishing a relationship on shear and curative properties.

REFERENCES

1. Stender, B.; Mantei, W.; Houbertz, R. From Lab to Fab -- High-Precision 3D Printing. *Laser Technik Journal.* **2017**, *14* (2), 20-23. https://onlinelibrary.wiley.com/doi/abs/10.1002/latj.201700009.
2. DBBP Design. 3D CAD Models. https://www.dbbpshop.com/?product_cat=various-parts (accessed April 15, 2021).
3. Dilberoglu, U. M.; Gharehpapagh, B.; Yaman, U.; Dolen, M. The Role of Additive Manufacturing in the Era of Industry 4.0. *Procedia Manuf.* **2017**, *11*, 545–554. https://doi.org/10.1016/j.promfg.2017.07.148.
4. Kodama, H. Automatic Method for Fabricating a Three-Dimensional Plastic Model with Photo-Hardening Polymer. *Rev. Sci. Instrum.* **1981**, *52* (11). https://aip.scitation.org/doi/abs/10.1063/1.1136492.
5. Melchels, F. Celebrating Three Decades of Stereolithography. *Virtual Phys. Prototyping*. **2012**, *7* (3), 173-175. https://doi.org/10.1080/17452759.2012.723408.
6. Formlabs. Validating Isotropy in SLA 3D Printing. https://formlabs.com/blog/isotropy-in-SLA-3D-printing/ (accessed April 15, 2021).
7. Berman, B. 3-D printing: The New Industrial Revolution. *Business Horizons.* **2012**, *55* (2), 155-162. https://www.sciencedirect.com/science/article/pii/S0007681311001790.

8. Geng, P.; Zhao, J.; Wu, W.; Ye, W.; Wang, Y.; Wang, S.; Zhang, S. Effects of Extrusion Speed and Printing Speed on the 3D Printing Stability of Extruded PEEK Filament. J. *Manuf. Technol. Processes.* **2019**, *37*, 266-273. https://www.sciencedirect.com/science/article/abs/pii/S1526612518301981.
9. Alharbi, N.; Osman, R.; Wismeijer, D. Effects of Build Direction on the Mechanical Properties of 3D-Printed Complete Coverage Interim Dental Restorations. *J. Prosthet. Dent*. **2016**, *115* (6), 760–767. https://doi.org/10.1016/j.prosdent.2015.12.002.
10. Duty, C. E.; Kunc, V.; Compton, B.; Post, B.; Erdman, D.; Smith, R.; Lind, R.; Lloyd, P.; Love, L. Structure and Mechanical Behavior of Big Area Additive Manufacturing (BAAM) Materials. *Rapid Prototyp. J*. 2017, *23* (1), 181–189. https://www.emerald.com/insight/content/doi/10.1108/RPJ-12-2015-0183/full/html.
11. Hadi, M. Surface Finish Effects Using Coating Method on 3D Printing (FDM) Parts. https://www.researchgate.net/figure/Schematic-diagram-of-FDM-4_fig1_324112415 (accessed April 15, 2021).
12. Carneiro, O.; Silva, A.; Gomes, R. Fused Deposition Modeling with Polypropylene. *Mater. Des*. **2015**, *83*, 768-776. https://www.sciencedirect.com/science/article/abs/pii/S0264127515004037?via%3Dihub.
13. Sood. A.; Ohdar, R.; Mahapatra, S. Parametric Appraisal of Mechanical Property of Fused Deposition Modelling Processed Parts. *Mater. Des*. **2010**, *31*, 287-295. https://www.sciencedirect.com/science/article/abs/pii/S0261306909002945.

14. Chockalingam, K.; Jawahar, N.; Chandrasekhar, U.; Praveen, J.; Karthic, M. Development of Process Model for Optimal Selection of Process Parameters for Geometric Tolerances and Surface Roughness in Stereolithography. *Int. J. Adv. Des. Manuf. Technol.* **2016**, 9 (3), 103-113. http://admt.iaumajlesi.ac.ir/article_534985.html.
15. Rios, O.; Carter, W.; Post, B.; Lloyd, P.; Fenn, D.; Kutchko, C.; Rock, R.; Olson, K.; Compton, B. 3D Printing via Ambient Reactive Extrusion. *Mater. Today Commun*. **2018**, *15*, 333–336. https://doi.org/10.1016/j.mtcomm.2018.02.031.
16. Soman, S. Study of Effects of Design Modification in Static Mixer Geometry and Its Applications. Master's Thesis. University of Waterloo, Ontario, Canada, 2016.
17. Akindoyo, O.; Beg, M.; Ghazali, S.; Islam, M.; Jeyaratnam, N.; Yuvaraj, A. Polyurethane Types, Synthesis and Applications-a Review. *RSC Adv*. **2016**, *6* (115), 114453– 114482. https://doi.org/10.1039/c6ra14525f.
18. Ning, L.; De-Ning, W.; Sheng-Kang, Y. Crystallinity and Hydrogen Bonding of Hard Segments in Segmented Poly(Urethane Urea) Copolymers. *Polymer (Guildf)*. **1996**, *37* (16), 3577–3583. https://doi.org/10.1016/0032-3861(96)00166-8.
19. Kébir, N.; Campistron, I.; Laguerre, A.; Pilard, J.; Bunel, C.; Couvercelle, J. Use of New Hydroxytelechelic cis-1,4-polyisoprene (HTPI) in the Synthesis of Polyurethanes (PUs): Influence of Isocyanate and Chain Extender Nature and their Equivalent Ratios on the Mechanical and Thermal Properties of PUs. *e-Polym.* **2013**, *6* (1). https://doi.org/10.1515/epoly.2006.6.1.619.

20. Molina, P.; Tárraga, A.; Arques, A. Synthesis: Carbon With Two Attached Heteroatoms With at Least One Carbon-to-Heteroatom Multiple Link. *Compr. Org. Funct. Group Transform. II.* **2005**, *5*, 949-973. https://doi.org/10.1016/B0-08-044655-8/00116-1.
21. Raftopoulos, K.; Janowski, B.; Apekis, L.; Pielichowski, K.; Pissis, P. Molecular Mobility and Crystallinity in Polytetramethylene Ether Glycol in the Bulk and as Soft Component in Polyurethanes. *Eur. Polym. J.* **2011**, *47* (11), 2120–2133. https://doi.org/10.1016/j.eurpolymj.2011.07.020.
22. Pukánszky B.; Bagdi, K.; Tóvölgyi, Z.; Varga, J.; Botz, L.; Hudak, S.; Dóczi, T.; Pukánszky, B. Nanophase Separation in Segmented Polyurethane Elastomers: Effect of Specific Interactions on Structure and Properties. *Eur. Polym. J.* **2008**, *44* (8), 2431-2438. https://www.sciencedirect.com/science/article/pii/S0014305708002802.
23. Arévalo-Alquichire, S.; Morales-Gonzalez, M.; Navas-Gómez, K.; Diaz, L.; Gómez-Tejedor, J.; Serrano, M.; Valero, M. Influence of Polyol/Crosslinker Blend Composition on Phase Separation and Thermo-Mechanical Properties of Polyurethane Thin Films. *Polymers*, **2020**, *12*, 666. https://doi.org/10.3390/polym12030666.